

Contents lists available at ScienceDirect

Gene

journal homepage: www.elsevier.com/locate/gene



Research paper

Genome-wide analysis of DNA methylation in five tissues of sika deer (*Cervus nippon*)[★]



Chun Yang^{a,b,1}, Yan Zhang^{c,1}, Wenyuan Liu^{a,b}, Xiao Lu^{a,b}, Chunyi Li^{a,b,*}

- ^a Institute of Special Wild Economic Animals and Plants, Chinese Academy of Agricultural Sciences, Changchun, PR China
- ^b State Key Laboratory for Molecular Biology of Special Economic Animals, Changchun, PR China
- ^c Key Laboratory of Jilin Province for Zoonosis Prevention and Control, Institute of Military Veterinary, Academy of Military Medical Sciences, Changchun, PR China

ARTICLE INFO

Keywords: DNA methylation Sika deer F-MSAP Tissue-specific differentially methylated regions (T-DMRs)

ABSTRACT

DNA methylation plays an important role in regulating gene expression during tissue development and differentiation in eukaryotes. In contrast to domestic animals, epigenetic studies have been seldom conducted in wild animals. In the present study, we conducted the genome-wide profiling of DNA methylation for five tissues of sika deer using the fluorescence-labeled methylation-sensitive amplified polymorphism (F-MSAP) technique. Overall, a total of 104,131 fragments were amplified including 41,951 methylated fragments using 32 pairs of selected primers. The average incidence of DNA methylation was approximately 38.18% in muscle, 40.32% in heart, 41.86% in liver, 41.20% in lung, and 41.68% in kidney, respectively. Also, the significant differences of the DNA methylation levels were found between the different tissue types (P < 0.05), which indicates that the differences of genome-wide DNA methylation levels may be related to gene expression during tissue development and differentiation. In addition, 37 tissue-specific differentially methylated regions (T-DMRs) were identified and recovered by MSAP in five tissues, and were further confirmed by Southern blot analysis. Our study presents the first look at the T-DMRs in sika deer and represents an initial step towards understanding of epigenetic regulatory mechanism underlying tissue development and differentiation in sika deer.

1. Introduction

DNA methylation is one of the main epigenetic modification mechanisms in eukaryotic genomes and is crucial for gene expression regulation during animal and plant development (Bird, 2002). It is performed by DNA methyltransferases (DNMT), which transfer a methyl group from an S-adenosylmethionine (SAM) to a cytosine in a CpG-dinucleotide sequence. Currently, a great deal of studies has shown that the DNA methylation has been implicated in various biological processes, including gene expression (Cedar, 1988), X chromosome inactivation (Allen et al., 1992), genomic imprinting (Hirose et al., 2013), development (Smith and Meissner, 2013), regeneration (Takayama et al., 2014) and disease (Argentieri et al., 2017).

DNA methylation is predominantly limited to CpG doublets, and methylation of CpG dinucleotides in the promoter and transcribed regions of genes often results in transcriptional inactivation, and some studies have shown that actively transcribed sequences are often

methylated less than promoters and certain coding regions of silent genes (Finnegan et al., 1993). The level of DNA methylation is correlated with differential gene expression among different tissue types, and significant differences in the levels or pattern of cytosine methylation have been observed in various tissues or under different functional states in the same tissue (Mandel and Chambon, 1979; Vanyushin, 2005). Some studies suggested that various levels of DNA methylation may regulate tissue-specific transcription (Grunau et al., 2000) and be important for normal development or differentiation (Schlosberg et al., 2017). For example, the neonatal murine heart is able to regenerate after severe injury, but changes in DNA methylation and gene expression patterns can influence heart regeneration (Jung et al., 2015). Therefore, the detection and analysis of levels and patterns of genome-wide DNA methylation in various tissues types is essential for understanding associations between tissue-specific methylation and tissue-specific gene expression.

In parallel with the significance in understanding the functional

Abbreviations: ABI, Applied Biosystems; AFLP, amplified fragment length polymorphism; CG, cytosine-guanine; MSAP, methylation sensitive amplification polymorphism; F-MSAP, fluorescent methylation sensitive amplification polymorphism; PCR, polymerase chain reaction; T-DMRs, Tissue-specific differentially methylated regions

^{*} Grant sponsor: National Natural Science Foundation of China: Grant number: 31402059

^{*} Corresponding author at: Institute of Special Wild Economic Animals and Plants, Chinese Academy of Agricultural Sciences, 4899 Juye Street, 130112, PR China.

¹ Chun Yang and Yan Zhang contributed to this work equally.

roles of DNA methylation, a convenient method for cytosine methylation detection should be used. In recently, there has been a series of methodological developments in profiling of genome-wide DNA methylation. However, most of them are entirely dependent on detailed knowledge of the genome sequence. The methylation sensitive amplified polymorphism (MSAP) method is a new modification of the classic amplification fragment length polymorphism (AFLP) technique (Vos et al., 1995), and depends on utilizing two different DNA methylationsensitive restriction isoschizomer pair HpaII and MspI (Reyna-Lopez et al., 1997). These enzymes recognize the same restriction site (CCGG), however, they have different sensitivities to certain methylation states of cytosine. HpaII is inactive if one or both cytosines are fully methylated (both strands are methylated) but cleaves the hemi-methylated sequence, whereas MspI is inactive if the external cytosine is fully or hemi-methylated (Vos et al., 1995). Currently, MSAP acts as a useful approach to detect whole genome-wide differentially methylated CCGG sites, especially for use with non-model organisms without detailed genome information (Herrera and Bazaga, 2010). Due to its reliability, intensity sensitivity, and convenient operation, the MSAP has been extensively applied to determine genomic DNA methylation levels and patterns in many species (Yang et al., 2011; Marconi et al., 2013; Tang et al., 2014; Zhao et al., 2015; Guevara et al., 2017). However, it should be noted that the methylation percentages calculated by MSAP are lower than the total absolute values at the CCGG sites because of the limitation of endonuclease enzyme cannot digest other unrecognized CCGG sites (Yaish et al., 2014). F-MSAP, an improvement of MSAP, is based on fluorescently labeled primers and capillary gel electrophoresis with an internal lane size standard instead of traditional denaturing acrylamide gel electrophoresis and silver staining (Yang et al., 2011). This method has been proven to be more sensitive, safer and more effective than the original MSAP (Wang et al., 2016).

In present study, we used F-MSAP method to screen and investigate the levels and patterns of cytosine methylation in five types of tissue from sika deer (muscle, heart, liver, lung and kidney). Furthermore, by comparing the data of F-MSAP and MSAP, we also isolated, sequenced and verified some fragments that are differentially methylated among different tissue types, which may be useful for further investigations into how methylation functions to regulate gene expression during tissue development and differentiation.

2. Materials and methods

2.1. Ethics statement

Animal experiments were performed in accordance with the guidelines on animal care and use established by Chinese Academy of Agricultural Sciences (CAAS) Animal Care and Use Committee.

2.2. Animal materials and genomic DNA preparation

Tissue from muscle (skeletal muscle), heart, liver, lung and kidney were collected separately from four 2-year-old healthy sika deer (2 \circlearrowleft and 2 \circlearrowleft). DNA extraction from 250 mg of each tissue was carried out by a DNeasy Blood&Tissue Kit (Qiagen, Germany) according to the manufacturer's protocols. The quality and concentration of DNA were measured by both agarose gel electrophoresis (1%) and spectrophotometric assays (Thermo Scientific NanoDrop 2000c, USA). The DNA samples were stored at $-20\,^{\circ}\text{C}$ until use.

2.3. Fluorescence-labeled methylation-sensitive amplified polymorphism (F-MSAP) assay

In the F-MSAP technique, the different methylation sensitive isoschizomers (*HpaII* and *MspI*) with an internal control restriction enzyme (*EcoRI*) were used for DNA digestion. The enzymatically digested products were then ligated to adaptors, and pre-amplification and selective

 Table 1

 Sequences of adapters and primers used in F-MSAP.

Adapters/primers	Sequence (5'-3')
EcoRI adapter	5'-CTCGTAGACTCGTACC-3'
	3'-CATCTGACGCATGGTTAA-5'
HpaII and MspI adapter	5'-GACGATGAGTCTAGAA-3'
	3'-CTACTCAGATCTTGC-5'
E + 1 primers (PreAmp)	5'-GACTGCGTACCAATTC + A-3'
HM + 1 primers (PreAmp)	5'-GATGAGTCTAGAAaCGG + T-3'
E + 3 primers	5'-GACTGCGTACCAATTC + AAC-3'
	5'-GACTGCGTACCAATTC + AAG-3'
	5'-GACTGCGTACCAATTC + ACA-3'
	5'-GACTGCGTACCAATTC + AGT-3'
	5'-GACTGCGTACCAATTC + ACT-3'
	5'-GACTGCGTACCAATTC + AGA-3'
	5'-GACTGCGTACCAATTC + ATG-3'
	5'-GACTGCGTACCAATTC + ATC-3'
HM + 3 primers	5'-FAM ^a -GATGAGTCTAGAACGG + TAA-3'
	5'-FAM-GATGAGTCTAGAACGG + TAT-3'
	5'-FAM-GATGAGTCTAGAACGG + TAG-3'
	5'-FAM-GATGAGTCTAGAACGG + TAG-3'

^a Primer was labeled with the blue fluorescent dye 5'-FAM (5'-carboxyfluorescein).

amplification with fluorescent labeled primers were performed. The amplified products were checked using capillary gel electrophoresis and sequenced by an ABI 3730xl DNA sequencer (Applied Biosystems, Foster, CA, USA). Only the clear and reproducible bands that appeared in three runs of independent PCR amplification were scored. The F-MSAP data were analyzed using Genescan3.1 software (Applied Biosystems). The adaptors and primers used in the present study were designed according to Yang et al. (2016), with minor modifications (Table 1). The detailed procedure was as follows.

2.4. DNA digestion and ligation

The Genomic DNA from each sample was digested with *EcoRI/HpaII* or *EcoRI/MspI* (Takara, Dalian, China); each resultant DNA fragment was ligated to adapters at 16 °C overnight. The digestion-ligation of each sample was performed in 25 μ l solution containing 250 ng DNA template, 3 U *EcoRI*, 3 U *HpaII* (or *MspI*), 1.5 U T4 DNA ligase (Takara, Dalian, China), 5 pmol *EcoRI* adapter, 50 pmol *HpaII/MspI* adapter and 2.5 μ l 10 × T4 ligase buffer. The mixture was incubated at 37 °C overnight and stored at -20 °C.

2.5. Pre-amplification PCR

Pre-amplification PCR was performed. It contained 2 µl of ligation products, 40 ng E + 1 primer, 40 ng H-M + 1 primer (Table 1), 0.5 U Ex Taq polymerase, 1.6 µl of dNTPs (2.5 mM), 1.2 µl of MgCl $_2$ (25 mM), 2 µl of $10\times$ PCR buffer and 14.1 µl of water. The PCR conditions were as follows: 94 °C for 5 min; 30 cycles of 94 °C for 30 s, 56 °C for 1 min and 72 °C for 1 min; and extension at 72 °C for 7 min prior to selective amplification. The PCR products from the pre-amplification were diluted to 1 to 25 (v:v) with water and stored at - 20 °C until use.

2.6. Selective amplification PCR

Selective amplifications were performed in 20 μ l solution containing 2 μ l of the diluted pre-amplification product, 10 ng E + 3 primer, 40 ng H-M + 3 primer labeled with fluorescence dye (Table 1), 0.5 U Ex Taq polymerase, 1.6 μ l of dNTPs (2.5 mM), 1.2 μ l of MgCl₂ (25 mM) and 2 μ l of 10 × PCR buffer. The PCR amplification reactions were performed using the touch-down cycles, and the conditions were as follows: 94 °C for 5 min; 13 touch-down cycles of 94 °C for 30 s, 65 °C (subsequently reduced each cycle by 0.7 °C) for 30 s and 72 °C for 1 min; 23 continued cycles of 94 °C for 30 s, 56 °C for 30 s and 72 °C for 1 min; and extension at 72 °C for 7 min. The Ex Taq polymerase buffers

Table 2
Methylation patterns of the *Hpa*II and *Msp*I digested genomic DNA.

Type	Methylation status	Sensitivity of	Sensitivity of enzymes		attern	Methylation status
		HpaII	MspI	Н	M	
I	CCGGC ^{5m} CGG GGCCGGCC	Active	Active	1	1	Unmethylation or inner methylation of single-stranded DNA
II	^{5m} CCGG GG ^{5m} CC	Active	Inactive	1	0	Hemi-methylation at the outer cytosine nucleotide in the CCGG sequence
III	C ^{5m} CGG GG ^{5m} CC	Inactive	Active	0	1	Full methylation of the internal CCGG

H and M indicate the enzyme combination of EcoRI/HpaII and EcoRI/MspI, respectively.

"1" band present; "0" band absent. 5m C is methylated.

were purchased from Takara.

2.7. Selective amplification products detection

An aliquot of $0.5\,\mu l$ of selective amplified products was added to $24.5\,\mu l$ of 70% cold ethanol, mixed and centrifuged at $3700\,rpm$ for $30\,min$ at $4\,^{\circ}C$, then collected the precipitate. Subsequently, the mixture of LIZ500 standard, HiDi and the precipitate was denatured at $94\,^{\circ}C$ for $10\,min$ and then was loaded onto a 4% denaturing gel. Finally, the bands were analyzed using Genescan $3.1\,software$. Three kinds of bands were detected and each test was repeated for three times (Table 2).

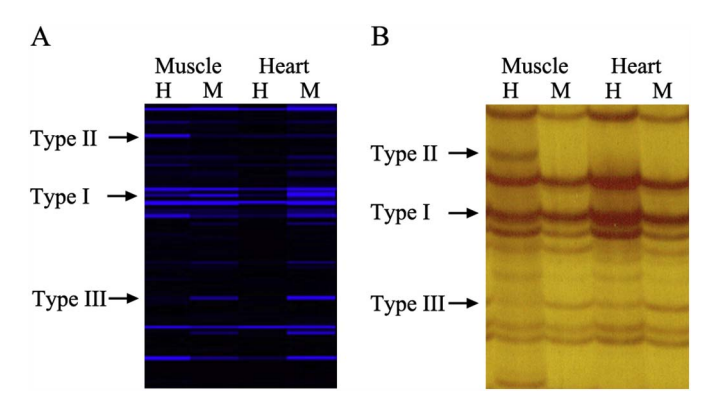
Based on the differential methylation sensitivity of isoschizomers, *Hpa*II and *Msp*I, cleaved band patterns were divided into three types (Fig. 1): Type I, which represents both bands for *Hpa*II and *Msp*I digestion, indicating no-methylation or inner methylation of single-stranded DNA. In order to simplify the analysis, Type I bands in our study were considered as no-methylation; Type II bands, which represent bands only for *Hpa*II digestion, indicating outer methylation of a single stranded DNA and hemi-methylation at the outer cytosine nucleotide in the CCGG sequence; Type III bands, which represent bands only for *Msp*I digestion, indicating inner methylation of double stranded DNA and full methylation of the CCGG sequence (Table 2).

The methylation ratio was calculated using the following formula:

$$\label{eq:methylation} \begin{split} \text{Methylation ratio} &= \text{Type II bands} + \text{Type III/Type I bands} \\ &+ \text{Type II bands} + \text{Type III bands} \end{split}$$

Full methylation ratio = Type III/Type I bands + Type II bands + Type III bands

Hemi - methylation ratio = Type II bands/Type I bands + Type II bands + Type III bands



 $\label{eq:Fig. 1. Cytosine methylation patterns with the primer combination HM + TAT/E + AAG. (A) The profile from F-MSAP; (B) The profile from MSAP using silver stain; H and M refer to digestion with $EcoRI/HpaII$ and $EcoRI/MspI$; Type I, Type II and Type III refer to unmethylated, hemi-methylated, and fully methylated sites, respectively.$

2.8. Cloning and sequencing of the T-DMRs

To isolate the T-DMRs fragments detected by F-MSAP, the same selected amplification products were detected by MSAP. The products denatured, separated by electrophoresis on a Long Ranger gel and stained with silver staining. Several fragments were excised directly from the wet polyacrylamide gels on the plate using a razor blade. The fragments were rehydrated with 50 µl of 95 °C ddH₂O for 5 min, slowly cooled down to room temperature, and centrifuged at 12,000g for 10 min. Supernatant of each sample was collected and 5 µl was used as the template for re-amplification. PCR reactions were performed with the same primer combinations and reaction conditions as those used in the selective amplification. After verification using a 1.8% agarose gel, the band was recovered using a gel extraction kit (Promega, Madison, USA) according to the manufacturer's instructions. Subsequently, the product was ligated into the vector pGM-T (TIANGEN, Beijing, China) and transformed into E. coli strain DH5α. The fragments were sequenced by SANGON (Shanghai, China). Homology search and sequence analysis were performed using the EMBL public database.

2.9. Southern blot analysis

Southern blot analysis was conducted to confirm the T-DMRs fragments. Primers were designed according to the sequence of the T-DMRs fragments and were labeled with DIG to prepare for the probe. Genomic DNA (20 μ g) was digested with EcoRI - HpaII or EcoRI - MspI, and each digestion product was electrophoresed on a 0.8% agarose gel in TBE and transferred onto Hybond-N + membranes (Promega). Probe labeling, transfer to membranes, fixation, hybridization and immunological detection were carried out according to the instructions of the DIG High Prime DNA Labeling and Detection Starter Kit II (Roche Applied Sciences, Mannheim, Germany). The probe was generated by PCR amplification of plasmid DNA. The PCR amplification system was the same as in the pre-amplification.

2.10. Statistical analysis

ANOVA and Duncan's multiple range tests were adopted for significance analysis of methylation levels among the different tissues through SPSS 18.0 software (SPSS, Inv., Chicago, IL). Statistical significance was set at P < 0.05. The hemi-methylation ratio (%), full methylation ratio (%), and total methylation ration (%) were calculated for each individual separately and analyzed by ANOVA, followed by Duncan's test.

3. Results

3.1. Genome-wide DNA methylation profiles of the different tissue types

Genome-wide DNA methylation profiles were generated for five tissue types of four sika deer individuals based on F-MSAP analysis. We

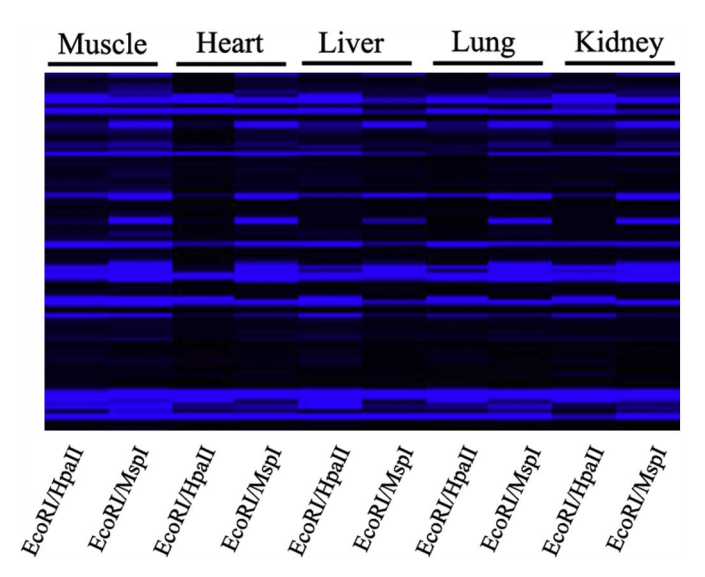


Fig. 2. Methylation profiles of the various tissue types using the combination of primers HM + TAT/E + AAG.

used 32 pairs of selected primers labeled with fluorescent dyes to detect genomic DNA methylation status in five tissue types. The F-MSAP profiles for the five tissues are shown in Fig. 2. A total of 20,962, 21,113, 21,250, 20,589 and 20,211 fragments were detected in muscle, heart, liver, lung and kidney, respectively. For each pair of primers, an average of 655, 660, 664, 643 and 663 fragments were amplified for each of above five tissue types, respectively. In particular, fragments between 100 bp and 300 bp were highly intense, and there were few fragments exceeding 500 bp.

3.2. DNA methylation patterns in the five tissue types

There cleavage patterns were defined in this study (see M + M section) and the results showed that the type I bands (unmethylated) were the most frequently observed representing 59.71% (62,180/10,4131) of the total. Type III bands made up 25.26% (26,294/10,4131) and the least frequent ones were type II bands being around 15.03% (15,657/10,4131). The sum of types II and III bands represents the methylated fragments and accounts for about 40.29% (41,951/10,4131) (Table 3).

Table 3
Methylation levels of cell group and tissue group.

3.3. DNA methylation levels in the five tissue types

For sika deer, different genome-wide DNA methylation levels in each tissue are shown in Table 3. The total methylated levels of genomic DNA in muscle, heart, liver, lung and kidney were $38.18\% \pm 2.67$, $40.32\% \pm 3.85$, $41.86\% \pm 2.99$, $41.20\% \pm 3.00$, $41.68\% \pm 2.77$, respectively. The hemi-methylated levels for each tissue type were $13.42\% \pm 1.39$, $13.94\% \pm 1.14$, $15.06\% \pm 1.14$, $14.75\% \pm 1.72$, $17.44\% \pm 1.88$, and the full-methylated levels were $24.76\% \pm 3.33$, $26.38\% \pm 3.61$, $26.26\% \pm 2.82$, $26.45\% \pm 4.05$ $24.24\% \pm 2.39$ for each tissue type of sika deer, respectively.

Analysis of variance and Duncan's multiple range tests were performed to evaluate the different methylation levels of various tissue types of sika deer (Table 3). There were no significant differences in DNA methylation level between heart, liver, lung and kidney (P > 0.05); However, the methylation level was significantly decreased in the muscle compared to the liver, lung and kidney (P < 0.05). In general, the genome-wide DNA methylation level in the muscle was the lowest among these tissue types, whereas the liver was highest.

3.4. Analysis of confirmation of the tissue-specific differentially methylated regions (T-DMRs)

The tissue-specific differentially methylated regions (T-DMRs) were identified by analysis of the differential DNA methylation patterns in five tissue types. Based on our studies, T-DMRs were defined as two types. Type I T-DMRs were defined as tissue-specific methylation fragments. Type II T-DMRs were defined as tissue-polymorphic methylation fragments. Comparing the profiles of F-MSAP and MSAP, a total of 37 T-DMRs were found, including four type I T-DMRs (T-DMR6, T-DMR26, T-DMR47 and T-DMR68) and thirty-three Type II T-DMRs, the details are shown in Table 4. The T-DMRs were further verified using methylation-sensitive Southern blot analysis with the isolated fragments as probes (Fig. 3). Through comparison with EMBL database, 37 T-DMRs had high similarity to characterized regions of the Bos Taurus genome. Fourteen of these 37 fragments were located within genes, five in the 3' downstream regions of the genes, twelve in the 5' upstream regions of the genes, and six not located in the genes (Table 5). In the fourteen located within genes, SFT2D1 is vesicle transport protein; B4GALT1 is galactosyltransferase, SHANK2 is an adapter protein, TNFSF11 and CHSY1 are play a role in osteogenesis, VAV3 and ANGPT2 are play a role in angiogenesis, RBM20 is RNAbinding protein, BCAP31 and Capr2 were involved in apoptosis,

Types	Tissues							
	Muscle	Heart	Liver	Lung	Kidney			
Unmethylated bands ¹	13,026	12,708	12,441	12,171	11,834			
Hemi-methylated bands	2816	2939	3303	3066	3533			
Fully methylated bands	5120	5466	5506	5358	4844			
Total amplified bands ²	20,962	21,113	21,250	20,595	20,211			
Total Methylated bands ³	7936	8405	8809	8424	8377			
Hemi-methylation ratio ⁴ (%)	$13.42^{a} \pm 1.39$	$13.94^{a} \pm 1.14$	$15.60^{\rm b} \pm 1.14$	$14.75^{\text{b}} \pm 1.72$	17.44° ± 1.88			
Full methylation ratio ⁵ (%)	$24.76^{a} \pm 3.33$	$26.38^{b} \pm 3.61$	$26.26^{b} \pm 2.82$	$26.45^{b} \pm 4.05$	$24.24^{a} \pm 2.39$			
Methylation ratio ⁶ (%)	$38.18^a \pm 2.67$	$40.32^{ab} \pm 3.85$	$41.86^{\text{b}} \pm 2.99$	$41.20^{\rm b} \pm 3.00$	$41.68^{b} \pm 2.2^{c}$			

Data represents mean \pm SD.

Data with different superscript letters (a, b and c) are significantly different at P < 0.05.

The number of bands is the sum of 3 individuals.

² Total amplified bands = Unmethylated bands + hemi-methylated bands + fully methylated bands.

 $^{^3}$ Total methylated bands = Hemi-methylated bands + fully methylated bands.

⁴ Hemimethylation ratio = Hemi-methylated bands/total amplified bands; the ratio was calculated for each individual separately and analyzed by ANOVA and Duncan's test. The statistic method was same with that for fully methylation ratio and methylation ratio.

⁵ Fully methylation ratio = Fully methylated bands/total amplified bands.

⁶ Methylation ratio = Total methylated bands/total amplified bands.

Table 4Tissue-specific methylation pattern of CCGG sites in the genome.

Type I	Isolated fragment		Pattern of bands in F-MSAP profile									
Type I T-DMR-6 0 0 0 0 0 1 0 1 0 0 0 0 1 1 T-DMR-26 1 0 1 0 1 0 1 0 1 0 1 1 0 T-DMR-47 1 0 1 0 1 0 1 0 0 0 0 0 0 0 0 T-DMR-47 1 0 0 1 0 1 0 0 0 0 0 0 0 0 0 0 0 0 0			Muscle		Heart		Liver		Lung		Kidney	
T-DMR-26			Н	M	Н	M	Н	M	Н	М	Н	M
T-DMR-47 1 0 1 0 1 0 0 0 0 0 1 0 0 0 0 0 0 0 0	Type I	T-DMR-6	0	0	0	0	0	1	0	0	0	0
T-DMR-68 0 0 0 1 0 0 0 0 0 0 0 0 0 0 0 0 0 0 0		T-DMR-26	1	0	1	0	1	0	1	0	1	1
Type II T-DMR-1 0 0 0 1 1 1 0 0 1 0 0 0 1 1 1 0 0 0 1 1 1 0 0 0 1 1 1 0 0 1 1 0 0 0 1 1 1 1 0 0 1 1 1 0 0 1 1 1 0 0 1 1 1 1 0 1		T-DMR-47	1	0	1	0	1	0	0	0	1	0
T-DMR-2 0 0 1 1 1 0 0 0 1 1 0 0 1 1 T-DMR-4 1 0 1 1 0 0 0 0 0 1 1 1 T-DMR-7 0 1 1 1 0 0 0 0 0 1 1 1 0 0 1 T-DMR-10 1 1 1 1 1 0 0 0 1 0 0 0 1 1 1 T-DMR-10 1 1 1 1 1 1 0 0 0 1 0 0 0 1 1 0 0 1 T-DMR-15 1 0 0 0 1 1 0 0 0 0 1 1 0 0 0 T-DMR-18 0 0 1 0 0 0 0 1 1 1 0 0 1 T-DMR-19 1 1 1 1 1 0 0 0 1 1 1 0 1 1 T-DMR-25 1 0 0 0 1 1 1 0 0 1 1 1 0 0 T-DMR-33 1 0 1 1 1 0 0 1 1 1 0 0 1 1 T-DMR-33 1 0 1 1 1 0 0 0 1 1 1 0 0 1 1 T-DMR-33 1 0 1 1 1 0 0 0 1 1 1 0 0 0 T-DMR-33 1 0 1 0 0 0 1 1 1 1 0 1 1 T-DMR-33 1 0 1 0 1 1 1 0 1 1 1 0 1 T-DMR-34 1 0 0 1 1 1 0 0 1 1 1 0 1 T-DMR-55 0 0 1 1 1 0 0 1 1 1 0 0 1 1 T-DMR-56 0 0 1 1 1 0 0 1 1 1 0 0 1 T-DMR-57 1 1 0 0 1 1 1 0 0 1 1 T-DMR-58 1 1 0 0 1 1 1 0 0 1 1 T-DMR-59 1 1 1 1 1 1 1 1 1 1 1 1 1 1 1 1 1 1 1		T-DMR-68	0	0	0	1	0	0	0	0	0	0
T-DMR-4 1 0 1 0 1 0 0 0 1 1 0 1 T-DMR-7 0 1 1 1 0 0 0 0 1 1 1 0 1 T-DMR-10 1 1 1 1 1 0 0 0 1 1 0 0 0 1 T-DMR-10 1 1 1 1 1 1 0 0 0 1 0 0 0 1 0 0 1 T-DMR-14 0 0 0 0 0 1 1 0 0 1 0 0 T-DMR-15 1 0 0 0 1 1 0 0 1 1 0 0 T-DMR-18 0 0 1 0 0 0 0 1 1 1 0 0 1 1 T-DMR-19 1 1 1 1 1 0 0 0 0 1 1 1 1 0 T-DMR-23 1 0 0 0 1 1 1 0 0 1 1 1 0 T-DMR-25 1 0 0 0 0 1 1 1 0 0 1 1 1 0 T-DMR-26 0 0 0 1 1 1 0 0 1 1 1 0 0 T-DMR-32 1 0 0 0 1 1 1 1 0 0 1 1 1 0 0 T-DMR-33 1 0 1 1 1 0 0 1 1 1 0 0 T-DMR-33 1 0 1 1 1 0 0 1 1 1 0 0 T-DMR-33 1 0 1 0 1 1 1 1 1 1 1 1 1 1 1 1 1 1 1	Type II	T-DMR-1	0	0	0	1	1	0	1	0	0	0
T-DMR-70		T-DMR-2	0	0	1	1	1	0	0	1	1	0
T-DMR-10		T-DMR-4	1	0	1	0	1	0	0	0	1	1
T-DMR-14 0 0 0 0 1 0 1 0 1 0 1 0 T-DMR-15 1 0 0 0 1 1 0 0 1 1 0 0 0 T-DMR-15 1 0 0 0 1 1 0 0 1 1 0 0 0 T-DMR-18 0 0 1 1 0 0 0 0 1 1 1 0 1 1 T-DMR-19 1 1 1 1 1 0 0 0 0 1 1 1 1 0 1 1 T-DMR-23 1 0 0 0 1 1 1 0 0 1 1 1 0 0 T-DMR-25 1 0 0 0 0 1 1 1 0 0 1 1 0 0 1 1 T-DMR-26 0 0 0 0 1 1 1 1 0 0 1 1 T-DMR-26 0 0 0 0 1 1 1 1 0 0 1 1 T-DMR-32 1 0 0 0 0 1 1 1 1 0 0 1 1 T-DMR-32 1 0 0 0 0 1 1 1 1 0 0 0 1 1 T-DMR-32 1 0 0 0 0 1 1 1 1 1 0 0 0 1 T-DMR-33 1 0 0 1 0 1 1 1 1 0 0 1 1 1 0 0 T-DMR-39 0 1 1 1 0 0 1 1 1 0 1 1 1 0 1 T-DMR-45 0 0 0 1 1 1 0 0 1 1 1 0 1 T-DMR-45 0 0 0 1 1 1 0 0 0 1 1 1 0 0 1 T-DMR-48 1 0 0 0 1 1 1 0 0 1 1 0 0 1 T-DMR-52 0 0 0 1 1 1 0 0 1 1 0 0 1 T-DMR-54 1 1 1 1 1 0 0 1 1 1 0 0 0 1 T-DMR-60 1 1 1 0 1 1 1 0 0 0 1 1 T-DMR-60 1 1 1 0 1 1 1 0 0 1 1 T-DMR-63 0 0 1 1 1 0 1 1 0 0 1 1 1 0 0 1 T-DMR-66 0 1 1 1 0 1 1 1 0 0 1 1 T-DMR-67 1 1 1 0 1 1 1 0 1 1 1 0 1 1 T-DMR-67 1 1 1 0 1 1 1 0 1 1 1 0 1 1 T-DMR-69 1 1 1 1 0 1 1 1 0 0 1 1 1 T-DMR-77 1 0 0 1 1 1 0 1 1 1 0 1 1 1 T-DMR-78 0 0 1 1 1 0 1 1 1 0 1 1 1 T-DMR-78 0 0 1 1 1 0 1 1 1 0 0 1 1 1 T-DMR-78 0 0 1 1 1 0 1 1 1 0 0 1 1 T-DMR-78 0 0 1 1 1 0 1 1 1 0 0 0 1 1 T-DMR-79 1 1 0 0 1 1 1 1 0 0 0 1 1 T-DMR-79 1 1 0 0 1 1 1 1 0 0 0 1 1 T-DMR-79 1 1 0 0 1 1 1 1 1 0 0 0 1 1 T-DMR-81 1 0 1 1 1 1 1 0 0 0 1 1 1 T-DMR-81 1 0 1 1 1 1 1 0 0 0 1 1 1 T-DMR-81 1 1 0 1 1 1 1 1 0 0 0 1 1 1 T-DMR-82 0 0 0 1 1 1 1 1 1 0 0 0 1 1 1 1 1 0 0 0 1 1 1 T-DMR-81 1 1 0 1 1 1 1 1 1 1 1 1 1 1 1 1 1 1 1		T-DMR-7	0	1	1	0	0	0	1	1	0	1
T-DMR-15		T-DMR-10	1	1	1	1	0	0	1	0	0	1
T-DMR-18 0 0 1 0 0 0 1 1 0 0 1 T-DMR-19 1 1 1 1 1 0 0 0 0 1 1 1 T-DMR-23 1 0 0 1 1 0 0 1 1 1 0 T-DMR-25 1 0 0 0 1 1 0 0 1 1 1 0 T-DMR-26 0 0 0 1 1 1 0 0 1 1 0 0 T-DMR-29 0 1 1 1 0 0 1 1 0 0 T-DMR-33 1 0 1 0 1 1 1 0 1 1 0 1 T-DMR-33 1 0 1 0 1 1 1 0 1 1 0 1 T-DMR-35 0 0 1 1 0 0 0 1 1 0 1 1 0 1 T-DMR-48 1 0 0 1 1 0 0 1 1 0 0 1 T-DMR-55 1 1 0 0 1 1 0 0 1 1 0 0 1 T-DMR-57 1 1 0 1 1 0 0 0 1 1 0 0 T-DMR-66 0 1 1 0 1 0 1 1 0 0 1 1 T-DMR-67 1 1 0 1 1 0 1 1 0 0 1 1 T-DMR-68 0 0 1 1 1 0 1 0 1 1 0 0 1 1 T-DMR-69 1 1 1 0 1 0 1 1 0 0 1 1 T-DMR-78 0 0 1 1 1 0 1 0 1 1 1 0 0 1 T-DMR-79 1 1 0 1 1 0 1 1 0 1 1 T-DMR-79 1 1 0 1 1 0 0 1 1 0 1 T-DMR-79 1 1 0 1 1 0 0 1 1 1 0 1 T-DMR-79 1 1 0 1 1 0 0 1 1 1 0 1 T-DMR-79 1 1 0 1 1 0 1 1 1 0 0 1 T-DMR-79 1 1 0 1 1 0 1 1 1 0 1 T-DMR-79 1 1 0 1 1 1 1 1 1 1 1 1 1 1 1 1 1 1 1 T-DMR-79 1 1 1 0 1 1 1 1 1 1 1 1 1 1 1 1 1 1 1		T-DMR-14	0	0	0	0	1	0	1	0	1	0
T-DMR-19		T-DMR-15	1	0	0	1	1	0	1	1	0	0
T-DMR-23 1 0 0 1 1 1 0 1 1 1 0 T-DMR-25 1 0 0 0 0 1 1 1 0 0 1 1 1 0 T-DMR-26 0 0 0 0 1 1 1 0 0 1 1 1 0 0 T-DMR-26 0 0 0 0 1 1 1 1 0 0 0 1 1 1 T-DMR-29 0 1 1 1 1 0 0 0 1 1 1 0 0 T-DMR-32 1 0 0 0 0 1 1 1 1 1 0 1 1 T-DMR-33 1 0 1 0 1 1 1 0 1 1 1 0 1 1 T-DMR-39 0 1 1 1 0 0 0 1 1 1 0 1 1 0 1 T-DMR-45 0 0 1 1 1 0 0 0 1 1 0 0 1 1 0 0 1 T-DMR-48 1 0 0 1 1 1 0 0 1 1 0 0 1 1 0 0 1 T-DMR-52 0 0 1 1 1 0 0 1 1 0 0 1 1 0 0 1 1 T-DMR-54 1 1 1 1 1 0 0 1 1 1 0 0 0 1 1 T-DMR-57 1 1 0 1 1 0 0 0 0 0 1 1 1 0 0 1 1 T-DMR-60 1 1 0 0 1 1 0 0 1 1 0 0 1 T-DMR-60 1 1 0 1 1 0 0 1 1 0 0 1 1 T-DMR-65 0 0 1 1 1 1 0 1 1 0 0 1 1 1 0 0 1 1 T-DMR-65 0 0 1 1 1 0 1 1 0 0 1 1 1 T-DMR-67 1 0 0 1 1 1 0 1 1 1 0 0 1 1 T-DMR-79 1 1 1 0 1 1 1 0 0 0 1 1 T-DMR-78 0 0 1 1 1 1 0 1 1 0 0 1 1 1 T-DMR-78 1 1 0 1 1 1 0 0 1 1 1 0 0 T-DMR-79 1 1 1 0 1 1 1 0 0 0 1 1 T-DMR-79 1 1 1 0 1 1 1 0 0 0 1 1 T-DMR-79 1 1 1 0 1 1 1 0 0 0 1 1 T-DMR-79 1 1 1 0 1 1 1 0 0 0 1 1 T-DMR-79 1 1 1 0 1 1 1 1 1 1 1 1 1 1 1 T-DMR-79 1 1 1 0 1 1 1 1 1 1 1 1 1 1 1 1 T-DMR-79 1 1 1 0 1 1 1 1 1 1 1 1 1 1 1 1 1 T-DMR-79 1 1 1 0 1 1 1 1 1 1 1 1 1 1 1 1 1 T-DMR-79 1 1 1 0 1 1 1 1 1 1 1 1 1 1 1 1 1 T-DMR-79 1 1 1 0 1 1 1 1 1 1 1 1 1 1 1 1 1 1 T-DMR-79 1 1 1 0 1 1 1 1 1 1 1 1 1 1 1 1 1 1 1		T-DMR-18	0	0	1	0	0	0	1	1	0	1
T-DMR-25		T-DMR-19	1	1	1	1	0	0	0	1	1	1
T-DMR-26 0 0 0 1 1 1 0 0 1 1 T-DMR-29 0 1 1 1 1 0 0 0 1 1 0 0 T-DMR-32 1 0 0 0 1 1 1 1 1 0 1 1 1 0 1 T-DMR-33 1 0 1 0 1 0 1 1 0 1 1 0 1 T-DMR-45 0 0 1 1 0 0 0 1 1 0 1 1 0 1 T-DMR-45 0 0 1 1 0 0 1 1 0 1 1 0 1 T-DMR-45 1 0 0 1 1 1 0 1 1 0 0 1 T-DMR-52 0 0 1 1 1 0 1 1 0 0 1 1 0 0 1 T-DMR-54 1 1 1 1 0 0 1 1 0 0 0 1 1 T-DMR-54 1 1 1 1 0 0 1 1 0 0 1 1 T-DMR-60 1 1 0 1 1 0 0 1 0 0 1 1 0 0 T-DMR-60 1 1 0 1 1 0 0 1 1 0 0 1 T-DMR-63 0 0 1 1 1 0 1 0 1 1 0 0 1 T-DMR-65 0 0 1 1 0 0 1 1 0 0 1 1 T-DMR-67 1 0 0 1 1 0 1 1 0 0 1 1 T-DMR-78 0 0 1 1 1 0 1 1 0 0 0 1 1 T-DMR-78 0 0 1 1 1 0 1 1 0 0 1 1 1 T-DMR-79 1 1 0 1 1 0 0 0 1 1 1 T-DMR-79 1 1 0 1 1 1 0 0 0 1 1 T-DMR-79 1 1 0 1 1 0 1 1 1 0 1 T-DMR-79 1 1 0 1 1 0 1 1 1 1 1 1 1 T-DMR-79 1 1 0 1 1 1 1 1 1 1 1 1 1 1 1 1 T-DMR-79 1 1 0 1 1 1 1 1 1 1 1 1 1 1 1 T-DMR-79 1 1 1 0 1 1 1 1 1 1 1 1 1 1 1 1 T-DMR-79 1 1 1 0 1 1 1 1 1 1 1 1 1 1		T-DMR-23	1	0	0	1	1	0	1	1	1	0
T-DMR-29 0 1 1 1 0 0 0 1 1 0 0 1 T-DMR-32 1 0 0 0 0 1 1 1 1 0 1 T-DMR-33 1 0 1 0 1 0 1 1 0 1 1 0 1 T-DMR-39 0 1 1 0 0 0 0 1 1 0 1 1 0 1 T-DMR-45 0 0 1 1 0 0 1 1 0 0 1 1 0 0 1 T-DMR-48 1 0 0 1 1 1 0 0 1 1 0 0 1 T-DMR-52 0 0 1 1 1 0 1 1 0 0 1 1 0 0 1 T-DMR-54 1 1 1 1 0 0 1 1 0 0 1 1 T-DMR-57 1 1 0 1 1 0 0 1 0 1 0 0 T-DMR-60 1 1 0 1 0 1 0 1 1 0 0 T-DMR-60 0 1 1 1 0 1 0 1 1 0 0 1 T-DMR-67 1 1 0 1 0 1 0 1 1 0 1 1 0 T-DMR-68 0 0 1 1 1 0 1 0 1 1 0 1 1 T-DMR-69 1 1 1 0 1 0 1 1 0 1 1 T-DMR-79 0 1 1 0 1 1 0 1 1 0 1 1 T-DMR-78 0 0 1 1 1 0 1 1 0 1 1 1 T-DMR-79 1 1 0 1 1 0 1 1 0 1 1 T-DMR-79 1 1 0 1 1 0 1 1 0 1 1 T-DMR-79 1 1 0 1 1 1 0 0 1 1 T-DMR-81 1 0 1 0 1 1 1 1 0 1 T-DMR-81 1 0 1 0 1 1 1 1 1 1 1 1 1 1 1 1 1 1 1		T-DMR-25	1	0	0	0	1	1	0	1	1	0
T-DMR-32		T-DMR-26	0	0	0	1	1	1	0	0	1	1
T-DMR-33 1 0 1 0 1 1 0 1 1 0 1 1 0 1 T-DMR-39 0 1 1 1 0 0 0 0 1 1 1 0 1 T-DMR-45 0 0 1 1 1 0 0 0 1 1 0 0 0 1 T-DMR-48 1 0 0 1 1 1 0 0 1 1 1 0 0 1 T-DMR-52 0 0 1 1 1 0 0 1 1 1 0 0 1 1 T-DMR-54 1 1 1 1 0 0 0 1 1 1 0 0 1 1 T-DMR-57 1 1 0 1 1 1 0 0 0 1 1 0 0 T-DMR-60 1 1 0 1 1 0 0 1 1 1 0 0 1 1 1 0 T-DMR-65 0 0 1 1 1 1 0 1 0 1 0 1 1 0 0 1 1 T-DMR-69 1 1 1 0 1 1 0 1 0 1 1 1 0 1 1 T-DMR-69 1 1 1 0 1 0 1 1 0 0 0 0 0 1 T-DMR-71 0 0 1 0 1 1 0 0 1 1 T-DMR-73 1 0 0 1 1 1 0 0 1 1 1 0 0 1 1 T-DMR-78 0 0 1 1 1 1 0 1 1 1 0 1 1 1 T-DMR-78 0 0 1 1 1 1 0 1 1 1 0 1 1 1 T-DMR-79 1 1 0 1 1 1 0 0 1 1 1 1 T-DMR-79 1 1 1 0 1 1 1 0 0 0 1 1 1 T-DMR-81 1 0 1 0 1 1 1 1 1 1 1 1 1 1 T-DMR-81 1 0 1 0 1 1 1 1 1 1 1 1 1 1 1 1 1 1 1		T-DMR-29	0	1	1	1	0	0	1	1	0	0
T-DMR-39 0 1 1 0 0 0 1 1 0 0 1 T-DMR-45 0 0 1 1 1 0 0 0 1 0 1 T-DMR-48 1 0 0 1 1 1 0 0 1 1 0 0 1 T-DMR-52 0 0 1 1 0 0 1 1 0 0 1 T-DMR-54 1 1 1 1 0 0 0 0 1 1 0 0 1 T-DMR-57 1 1 0 1 1 0 0 1 1 0 0 T-DMR-60 1 1 0 1 0 1 0 0 1 1 0 T-DMR-63 0 0 1 1 1 0 1 0 0 1 0 0 1 T-DMR-65 0 0 1 1 0 1 0 0 0 0 0 1 T-DMR-69 1 1 1 0 1 0 1 0 0 0 0 0 1 T-DMR-79 1 1 0 1 1 0 1 1 0 0 1 1 1 T-DMR-75 0 1 1 0 1 1 0 0 0 0 0 0 1 T-DMR-79 1 1 0 1 1 0 0 1 1 0 1 1 1 T-DMR-79 1 1 0 1 1 0 0 1 1 1 1 1 T-DMR-81 1 0 1 0 1 1 1 1 1 1 1 T-DMR-81 1 0 1 0 1 1 1 1 1 1 1 T-DMR-82 0 0 1 1 1 1 1 0 1 1 1 1		T-DMR-32	1	0	0	0	1	1	1	1	0	1
T-DMR-45 0 0 1 1 0 0 1 0 0 1 T-DMR-48 1 0 0 1 1 1 0 0 1 1 0 0 1 T-DMR-52 0 0 1 1 1 0 0 1 1 0 0 1 T-DMR-54 1 1 1 1 1 0 0 0 0 1 1 T-DMR-57 1 1 0 1 1 0 0 1 0 1 0 T-DMR-60 1 1 0 1 0 1 0 1 1 0 T-DMR-63 0 0 1 1 1 0 1 1 0 1 1 0 0 1 T-DMR-65 0 0 1 1 1 0 1 1 0 1 1 0 1 1 T-DMR-71 0 0 1 0 1 0 1 1 0 1 1 T-DMR-75 0 1 1 1 0 1 1 0 0 0 1 1 T-DMR-75 0 1 1 1 0 1 1 0 0 0 1 1 T-DMR-78 0 0 1 1 1 0 1 1 0 1 1 0 T-DMR-79 1 1 0 1 1 0 0 1 1 1 0 1 T-DMR-79 1 1 0 1 1 0 0 1 1 T-DMR-81 1 0 1 0 1 1 1 0 1 1 T-DMR-81 1 0 1 0 1 1 1 0 1 1 T-DMR-81 1 0 1 0 1 1 1 1 1 1		T-DMR-33	1	0	1	0	1	1	0	1	1	0
T-DMR-48 1 0 0 1 1 1 0 1 0 0 1 1 T-DMR-52 0 0 1 1 1 0 0 1 1 0 0 1 1 T-DMR-52 0 0 1 1 1 0 0 1 1 0 0 1 1 T-DMR-54 1 1 1 1 1 0 0 0 0 0 0 0 1 1 T-DMR-57 1 1 0 1 1 0 0 1 0 0 1 0 0 T-DMR-60 1 1 0 1 0 1 0 1 1 0 0 1 1 0 0 T-DMR-63 0 0 1 1 1 0 0 1 1 0 0 1 1 T-DMR-65 0 0 1 1 1 0 1 1 0 0 1 1 T-DMR-69 1 1 1 0 1 0 1 0 0 0 0 0 1 T-DMR-71 0 0 1 0 1 1 0 0 0 1 1 T-DMR-73 1 0 0 1 1 1 1 0 0 1 1 1 T-DMR-75 0 1 1 1 0 1 1 0 0 1 1 1 T-DMR-78 0 0 1 1 1 0 0 1 1 1 0 0 1 1 T-DMR-78 0 0 1 1 1 1 0 0 1 1 1 0 0 T-DMR-79 1 1 0 1 1 0 1 1 1 0 0 1 1 T-DMR-79 1 1 0 1 1 1 0 0 1 1 1 T-DMR-81 1 0 1 0 1 1 1 1 0 1 1 T-DMR-81 1 0 1 0 1 1 1 1 0 0 1 1 1 T-DMR-81 1 0 1 1 1 1 0 0 1 1 1 1 1 1 0 1 1 T-DMR-82 0 0 0 1 1 1 1 1 0 0 1 1 1 1 1		T-DMR-39	0	1	1	0	0	0	1	1	0	1
T-DMR-52 0 0 1 1 0 0 1 1 0 0 1 T-DMR-54 1 1 1 1 1 0 0 0 0 0 1 1 T-DMR-57 1 1 0 1 1 0 0 1 0 1 0 0 T-DMR-60 1 1 0 1 0 1 0 1 1 0 0 1 T-DMR-63 0 0 1 1 1 0 1 0 1 0 1 1 0 0 T-DMR-65 0 0 1 1 0 1 1 0 1 0 1 1 1 T-DMR-69 1 1 1 0 1 0 1 0 0 0 1 1 T-DMR-71 0 0 1 0 1 1 0 0 1 1 T-DMR-78 0 0 1 1 1 0 1 0 0 1 1 T-DMR-78 0 0 1 1 1 0 1 0 0 1 1 1 T-DMR-79 1 1 0 1 1 0 0 1 1 0 0 1 1 T-DMR-81 1 0 1 0 1 1 1 0 0 1 1 T-DMR-82 0 0 1 1 1 1 1 0 0 1 1		T-DMR-45	0	0	1	1	0	0	1	0	0	1
T-DMR-54		T-DMR-48	1	0	0	1	1	1	0	1	1	0
T-DMR-57		T-DMR-52	0	0	1	1	0	1	1	0	0	1
T-DMR-60 1 1 0 1 0 1 0 1 1 0 1 1 0 1 T-DMR-63 0 0 1 1 1 1 0 1 0 1 0 1 1 1 T-DMR-65 0 0 1 1 1 0 1 0 0 1 1 T-DMR-65 0 0 1 1 1 0 0 1 1 0 0 0 1 1 T-DMR-71 0 0 1 0 1 1 0 0 0 1 1 T-DMR-73 1 0 0 1 1 1 0 0 1 1 1 1 T-DMR-75 0 1 1 0 1 1 0 1 1 1 0 1 1 1 T-DMR-78 0 0 1 1 1 0 0 1 1 0 0 0 0 T-DMR-79 1 1 0 1 1 0 0 0 1 1 T-DMR-81 1 0 1 1 1 1 1 1 1 1 1 1 1 1 1 1 1 1 1		T-DMR-54	1	1	1	1	0	0	0	0	1	1
T-DMR-63 0 0 1 1 1 0 1 0 0 1 T-DMR-65 0 0 1 1 0 1 0 1 1 1 T-DMR-69 1 1 1 0 1 0 0 0 0 1 T-DMR-71 0 0 1 0 1 1 0 0 1 1 T-DMR-73 1 0 0 1 1 1 0 1 1 1 1 T-DMR-75 0 1 1 0 1 1 0 1 1 0 1 1 1 T-DMR-78 0 0 1 1 1 0 0 1 1 0 0 0 0 T-DMR-79 1 1 0 1 1 0 0 0 1 1 T-DMR-81 1 0 1 0 1 1 1 1 0 1 T-DMR-82 0 0 1 1 1 1 0 0 1 1 1		T-DMR-57	1	1	0	1	1	0	0	1	0	0
T-DMR-65 0 0 1 1 0 1 1 0 1 1 T-DMR-69 1 1 1 0 1 1 0 0 0 0 0 1 T-DMR-71 0 0 1 0 1 1 0 0 0 0 1 1 T-DMR-73 1 0 0 1 1 1 1 0 1 1 1 0 1 1 1 T-DMR-75 0 1 1 1 0 1 1 0 1 1 1 0 T-DMR-78 0 0 1 1 1 1 0 0 1 1 0 0 T-DMR-79 1 1 0 1 1 0 0 0 1 1 T-DMR-81 1 0 1 0 1 1 1 1 1 1 1 1 1 1 1 1 1 1 1		T-DMR-60	1	1	0	1	0	1	0	1	1	0
T-DMR-69 1 1 1 0 1 0 0 0 0 1 T-DMR-71 0 0 1 0 1 1 0 0 0 1 1 1 T-DMR-73 1 0 0 1 1 1 1 0 1 1 1 1 1 T-DMR-75 0 1 1 1 0 1 1 1 0 1 1 1 0 T-DMR-78 0 0 1 1 1 1 0 0 1 1 0 0 T-DMR-79 1 1 0 1 1 0 0 0 1 1 1 T-DMR-81 1 0 1 0 1 1 1 1 1 1 1 1 1 1 1 1 1 1 1		T-DMR-63	0	0	1	1	1	0	1	0	0	1
T-DMR-71 0 0 1 0 1 1 0 0 1 1 1 T-DMR-73 1 0 0 1 1 1 0 0 1 1 1 1 T-DMR-75 0 1 1 1 0 1 1 0 1 1 1 0 T-DMR-78 0 0 1 1 1 1 0 0 1 1 0 0 T-DMR-79 1 1 0 1 1 0 0 0 1 1 T-DMR-81 1 0 1 0 1 1 1 1 0 0 1 1 T-DMR-82 0 0 1 1 1 1 0 0 1 1 1 1 1 1 1 1 1 1 1		T-DMR-65	0	0	1	1	0	1	1	0	1	1
T-DMR-73 1 0 0 1 1 1 0 1 1 1 T-DMR-75 0 1 1 1 0 1 1 0 1 1 0 0 1 1 0 0 1 1 1 0 0 1 1 1 0 0 1 1 1 0 0 1 1 1 0 0 1 1 1 0 0 0 1 1 1 1 0 0 0 0 1 1 1 1 1 0 0 0 0 1		T-DMR-69	1	1	1	0	1	0	0	0	0	1
T-DMR-75 0 1 1 0 1 1 0 1 1 0 T-DMR-78 0 0 1 1 1 0 0 1 0 0 T-DMR-79 1 1 0 1 1 0 0 0 1 1 T-DMR-81 1 0 1 0 1 1 1 1 1 0 1 T-DMR-82 0 0 1 1 1 1 0 0 1 1 1		T-DMR-71	0	0	1	0	1	1	0	0	1	1
T-DMR-78 0 0 1 1 1 0 0 1 0 0 T-DMR-79 1 1 0 1 1 0 0 0 1 1 T-DMR-81 1 0 1 0 1 1 1 1 0 1 T-DMR-82 0 0 1 1 1 1 0 0 1 1 1 1		T-DMR-73	1	0	0	1	1	1	0	1	1	1
T-DMR-79 1 1 0 1 1 0 0 0 1 1 T-DMR-81 1 0 1 0 1 1 1 0 0 1 T-DMR-82 0 0 1 1 1 0 0 1 1		T-DMR-75	0	1	1	0	1	1	0	1	1	0
T-DMR-81 1 0 1 0 1 1 1 1 0 1 T-DMR-82 0 0 1 1 1 0 0 1 1 1		T-DMR-78	0	0	1	1	1	0	0	1	0	0
T-DMR-81 1 0 1 0 1 1 1 1 0 1 T-DMR-82 0 0 1 1 1 0 0 1 1 1		T-DMR-79	1	1	0	1	1	0	0	0	1	1
T-DMR-82 0 0 1 1 1 0 0 1 1 1		T-DMR-81	1	0	1	0	1	1	1	1	0	1
			0	0	1		1	0		1	1	1
			0	0	1	0	0	1	1	1	0	1

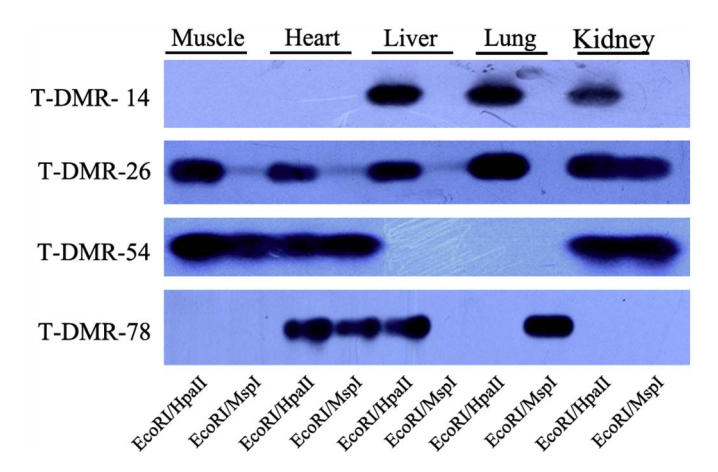


Fig. 3. Confirmation of the tissue-specific differentially methylated regions (T-DMRs); hybridization using T-DMR-14; hybridization using T-DMR-26; hybridization using T-DMR-78.

SULT1C3 is sulfotransferase, KMT2C is histone methyltransferase, CYP4A22 is cytochrome P450, VWF is von Willebrand factor. The detail description and function of the fourteen genes are shown in Table 6.

Table 5
Sequence analysis of all tissue-specific differentially methylation regions (T-DMRs).

Fragment	Size (bp)	Chromosome	Location	Gene	Id%
T-DMR-1	100	3	5' side	SNX29	95
T-DMR-2	259	1	Within	SFT2D1	96
T-DMR-4	144	9	NO		95
T-DMR-6	124	8	Within	B4GALT1	98
T-DMR-7	178	10	5' side	GALC	91
T-DMR-10	190	11	Within	SHNAK2	95
T-DMR-14	194	13	3' side	SNORA25	96
T-DMR-15	188	10	NO		91
T-DMR-17	157	17	5' side	ZDHHC8	91
T-DMR-18	165	15	Within	TNFSF11	96
T-DMR-19	120	4	Within	VAV3	98
T-DMR-23	249	14	Within	RBM2O	97
T-DMR-25	107	9	5' side	DDX43	93
T-DMR-26	70	1	3' side	ZPLD	89
T-DMR-29	137	X	Within	BACP31	95
T-DMR-32	195	21	Within	CHSY1	96
T-DMR-33	321	11	Within	SULT1C3	95
T-DMR-39	179	12	5' side	LPO	92
T-DMR-45	130	6	NO		94
T-DMR-47	96	4	5' side	CD2	87
T-DMR-48	100	16	NO		91
T-DMR-52	181	13	3' side	DHX8	94
T-DMR-54	287	4	Within	KMT2C	97
T-DMR-57	205	20	5' side	NDUFS4	93
T-DMR-60	213	23	3' side	KCNK16	94
T-DMR-63	210	3	Within	CYP4A22	93
T-DMR-65	160	3	5' side	HIVEP3	96
T-DMR-68	118	5	Within	CAPRIN2	90
T-DMR-69	245	29	5' side	NTM	94
T-DMR-71	110	27	Within	ANGPT2	90
T-DMR-73	98	16	NO		89
T-DMR-75	168	1	5' side	SETD4	94
T-DMR-78	82	22	3' side	OXTR	93
T-DMR-79	121	9	NO		90
T-DMR-81	123	5	Within	VWF	89
T-DMR-82	237	X	5' side	KAL1	86
T-DMR-86	104	15	5' side	ALKBH8	90

4. Discussion

MSAP is a modified AFLP technique, which has been widely applied in detecting large scale changes in genomic methylation in plants and animals, and has proven to be a highly efficient and powerful tool for investigating DNA methylation in various species in recent years (Sha et al., 2005; Xu et al., 2007). Depending on the different methylation sensitivity of isoschizomers, this approach makes it possible to study genome-wide DNA methylation on species without a fully sequenced genome. Thus, the F-MSAP method would be preferable for safety, efficiency and high resolution to previously described MSAP detection method (Yang et al., 2011). In the present study, we used F-MSAP method to detect genomic DNA methylation in various tissues of the sika deer. Our results indicated that DNA methylation exists in each tissue type of sika deer. There were no significant differences in DNA methylation level between heart, liver, lung and kidney (P > 0.05), but the DNA methylation level was significantly decreased in the muscle compared to the liver, lung and kidney (P < 0.05). Using F-MSAP technique, many studies have revealed the differential of genome-wide DNA methylation levels which were often displayed among different tissue types in different organisms. For instance, genome-wide DNA methylation level ranges from 26.1% to 29.4% in chicken (Xu et al., 2007), from 50.18% to 53.99% in swine (Yang et al., 2011) and from 27.61% to 56.25% in sea cucumber (Zhao et al., 2015). Our results are consistent with chicken (Xu et al., 2007) and sea cucumber (Zhao et al., 2015). Otherwise, in DNA methylation patterns, the full-methylation sites (type III) occur more frequently than hemimethylation sites (type II) in the five tissue types detected in this study, which is consistent with deer antler (Yang et al., 2016) and sea

Table 6
The description and function of fourteen genes.

Gene	Protein-coding	Function
SFT2D1	Vesicle transport protein SFT2A	May be involved in fusion of retrograde transport vesicles derived from an endocytic compartment with the Golgi complex.
B4GALT1	Beta-1,4-galactosyltransferase 1	Protein glycosylation.
SHANK2	SH3 and multiple Ankyrin repeat domains protein 2	Play a role in the structural and functional organization of the dendritic spine and synaptic junction.
TNFSF11	Tumor necrosis factor ligand superfamily member 11	Induces osteoclast-specific gene transcription to allow differentiation of osteoclasts.
VAV3	Guanine nucleotide exchange factor VAV3	Play an important role in angiogenesis.
RBM20	RNA-binding protein 20	As a regulator of mRNA splicing of a subset of genes involved in cardiac development.
BCAP31	B-cell receptor-associated protein 31	May be involved in CASP8-mediated apoptosis.
CHSY1	Chondroitin sulfate synthase1	Play a role in the negative control of osteogenesis.
SULT1C3	Sulfotransferase 1C3	Catalyze the sulfate conjugation of xenobiotic compounds and endogenous substrates.
KMT2C	Histone-lysine N-methyltransferase 2C	May be involved in leukemogenesis and developmental disorder.
CYP4A22	Cytochrome P450 4A22	Catalyzes the omega- and (omega-1)-hydroxylation of various fatty acids.
Capr2	Caprin-2	Involved in apoptosis.
ANGPT2	Angiopoietin-2	May facilitate endothelial cell migration and proliferation, thus serving as a permissive angiogenic signal.
VWF	Von Willebrand factor	Important in the maintenance of hemostasis, it promotes adhesion of platelets to the sites of vascular injury by forming a molecular bridge between sub-endothelial collagen matrix and platelet-surface receptor complex GPIb-IX-V.

cucumber (Zhao et al., 2015). However, the DNA methylation patterns of genome observed in present study appears to be different from some domestic animals (Xu et al., 2007; Yang et al., 2011), this discrepancies may result from different genetic backgrounds, species or different methods of methylation detection, which are likely to exhibit different DNA methylation levels and patterns (Kerkel et al., 2008; Boks et al., 2009; Schalkwyk et al., 2010; Zhang et al., 2010). Moreover, different tissues within the same species were also exhibited differences in DNA methylation levels and patterns. DNA demethylation plays a pivotal role in shaping DNA methylation levels and patterns, but the underlying mechanisms are still incompletely understood (Bhutani et al., 2011; Nabel et al., 2012; Kohli and Zhang, 2013). In generally, DNA demethylation can occur through passive pathway and active pathway (Bhutani et al., 2011). Passive DNA demethylation refers to the loss of the methyl group from 5-methylcytosine when DNA methyltransferase 1 (DNMT1) is inhibited or absent during successive rounds of DNA replication (Franchini et al., 2012). Active DNA demethylation is an enzymatic process (Gadd45, MBD4, TDG and TET) (Niehrs and Schafer, 2012). Therefore, dynamics of this process could also lead to the observed genome-wide DNA methylation levels and patterns diversity.

The different DNA methylation levels and patterns in various tissue types were possibly related to the regulatory mechanism of gene expression during tissue differentiation and developmental processes (Lu et al., 2008; Sharma et al., 2009). Some studies have demonstrated that some genes were characterized by their variable levels of methylation in different tissues, and under methylation in these genes in general correlated with tissue-specific gene expression (Futscher et al., 2002). At the same time, there are some studies expressing doubts on the correlation between gene expression and methylation regulation (Walsh and Bestor, 1999). At present, the main studies regarding DNA methylation regulation have focused on the promoter regions of genes and found that, if the gene promoter is hypermethylated or hypomethylated, then the gene may be silenced or activated accordingly (Shen et al., 2012; Sharma et al., 2017). In addition, it should be noted that cytosine-methylated CCGG sequences are distributed in repetitive sequences in the coding and noncoding regions that contain introns, repetitive elements, and potentially active transposable elements (Saze and Kakutani, 2011). In this study, we found that among 37 sites of T-DMRs, the sequence ranged from 70 to 321 bp. Fourteen were located within introns, twelve in the 5' upstream regions of genes, and five in the 3' downstream regions of genes. Moreover, because the sika deer genome is not currently available, we could not locate six sites in genes, but could only locate them at the chromosome level. The genes that contain these T-DMRs may be related to tissue development and

differentiation, and thus constitute a core set of epi-marker resource that would facilitate further epigenetic studies in tissue development and differentiation, or other biological processes.

Among these T-DMRs, the one that was localized in the gene RMB20 was only not detected in the heart. RMB20, a gene encoding a RNAbinding protein (RBP), is a critical regulator of cardiac function through its action on titin and tropomyosin (Guo et al., 2012). Loss-of-function mutations for RBM20 have been identified in 1.9%-3% of individuals with idiopathic dilated cardiomyopathy (Brauch et al., 2009; Guo et al., 2012). Conserved throughout evolution, compelling evidence has established RBPs with cardiac function and development processed. Fox example, RBM24 was recently demonstrated to be enriched in embryonic stem cells (ESC) derived cardiomyocytes and required for sarcomere assembly and heart contractility (Poon et al., 2012). In addition, Hermes was found to regulated heart development in Xenopus (Gerber et al., 2002). Therefore, RBM20 is an essential component of the RNA processing machinery during cardiogenesis and it is required in regulating cardiac gene expression of patterning normal structural and physiological integrity of newly formed cardiomyocytes and physiological integrity of newly formed cardiomyocytes (Beraldi et al., 2014). Likewise, a T-DMR of the gene SHANK2 was only not detected in the liver. SHANK2 is a member of the Shank family, which consists of important scaffolding proteins (SHANK1, SHANK2, and SHANK3) of postsynaptic density (Baron and Schattschneider, 2006; Grabrucker et al., 2011). It is reported that expression of SHANK2 is mainly associated with the development of the nerve system during embryogenesis (Gessert et al., 2011). It is well known that liver is a type of unusual tissue in that it only contains sympathetic nerves. The sensory nerves do not directly innervate hepatocytes, but are restricted to the stroma surrounding triades of hepatic vasculature and bile ducts, and to extrahepatic portions of the portal vein and bile ducts (Berthoud, 2004). Currently, we do not know whether the SHANK family stimulates or inhibits different types of nerve fibers, and if they do, methylation of the SHANK2 gene might induce growth of sensory nerves into other tissues during development.

The tissue development and differentiation is a complex biological process and may be controlled by many genes which are regulated by DNA methylation. In future studies, we would like to verify whether the genes that include the methylated sites found in this study are associated with tissue development and differentiation, which will help to reveal the underlying molecular mechanisms of tissue development and differentiation.

5. Conclusions

In the present study, genome-wide profiling of DNA methylation was conducted for the five tissue types of sika deer using F-MSAP technique. The different DNA methylation levels and patterns within tissues were evaluated, and significant differences in the genome-wide DNA methylation levels were demonstrated between various tissue types in sika deer. Our study presents the first look at the tissue-specific differentially methylated regions (T-DMRs) in sika deer. Based on the findings from this study and the functions on the gene expression, we think that differences in the DNA methylation levels and patterns may be important to regulate tissue-specific gene expression; however, a much more extensive analysis will be required to confirm this.

Acknowledgements

This work was supported by National Natural Science Foundation of China (Grant No. 31402059).

References

- Allen, R.C., Zoghbi, H.Y., Moseley, A.B., Rosenblatt, H.M., Belmont, J.W., 1992. Methylation of HpaII and HhaI sites near the polymorphic CAG repeat in the human androgen-receptor gene correlates with X chromosome inactivation. Am. J. Hum. Genet. 51, 1229–1239.
- Argentieri, M.A., Nagarajan, S., Seddighzadeh, B., Baccarelli, A.A., Shields, A.E., 2017. Epigenetic pathways in human disease: the impact of DNA methylation on stress-related pathogenesis and current challenges in biomarker development. EBioMedicine 18, 327–350.
- Baron, R., Schattschneider, J., 2006. Chapter 25 the autonomic nervous system and pain. Handb. Clin. Neurol. 81, 363–382.
- Beraldi, R., Li, X., Martinez Fernandez, A., Reyes, S., Secreto, F., Terzic, A., Olson, T.M., Nelson, T.J., 2014. Rbm20-deficient cardiogenesis reveals early disruption of RNA processing and sarcomere remodeling establishing a developmental etiology for dilated cardiomyopathy. Hum. Mol. Genet. 23, 3779–3791.
- Berthoud, H.R., 2004. Anatomy and function of sensory hepatic nerves. Anat. Rec. A Discov. Mol. Cell. Evol. Biol. 280, 827–835.
- Bhutani, N., Burns, D.M., Blau, H.M., 2011. DNA demethylation dynamics. Cell 146, 866–872.
- Bird, A., 2002. DNA methylation patterns and epigenetic memory. Genes Dev. 16, 6–21.Boks, M.P., Derks, E.M., Weisenberger, D.J., Strengman, E., Janson, E., Sommer, I.E., Kahn, R.S., Ophoff, R.A., 2009. The relationship of DNA methylation with age, gender and genotype in twins and healthy controls. PLoS One 4, e6767.
- Brauch, K.M., Karst, M.L., Herron, K.J., de Andrade, M., Pellikka, P.A., Rodeheffer, R.J., Michels, V.V., Olson, T.M., 2009. Mutations in ribonucleic acid binding protein gene cause familial dilated cardiomyopathy. J. Am. Coll. Cardiol. 54, 930–941.
- Cedar, H., 1988. DNA methylation and gene activity. Cell 53, 3-4.
- Finnegan, E.J., Brettell, R.I., Dennis, E.S., 1993. The role of DNA methylation in the regulation of plant gene expression. EXS 64, 218–261.
- Franchini, D.M., Schmitz, K.M., Petersen-Mahrt, S.K., 2012. 5-Methylcytosine DNA demethylation: more than losing a methyl group. Annu. Rev. Genet. 46, 419–441. Futscher, B.W., Oshiro, M.M., Wozniak, R.J., Holtan, N., Hanigan, C.L., Duan, H.,
- Futscher, B.W., Oshiro, M.M., Wozniak, R.J., Holtan, N., Hanigan, C.L., Duan, H., Domann, F.E., 2002. Role for DNA methylation in the control of cell type specific maspin expression. Nat. Genet. 31, 175–179.
- Gerber, W.V., Vokes, S.A., Zearfoss, N.R., Krieg, P.A., 2002. A role for the RNA-binding protein, hermes, in the regulation of heart development. Dev. Biol. 247, 116–126.
- Gessert, S., Schmeisser, M.J., Tao, S., Boeckers, T.M., Kuhl, M., 2011. The spatio-temporal expression of ProSAP/shank family members and their interaction partner LAPSER1 during *Xenopus laevis* development. Dev. Dyn. 240, 1528–1536.
 Grabrucker, A.M., Schmeisser, M.J., Udvardi, P.T., Arons, M., Schoen, M., Woodling, N.S.,
- Grabrucker, A.M., Schmeisser, M.J., Udvardi, P.T., Arons, M., Schoen, M., Woodling, N.S., Andreasson, K.I., Hof, P.R., Buxbaum, J.D., Garner, C.C., Boeckers, T.M., 2011. Amyloid beta protein-induced zinc sequestration leads to synaptic loss via dysregulation of the ProSAP2/Shank3 scaffold. Mol. Neurodegener. 6, 65.
- Grunau, C., Hindermann, W., Rosenthal, A., 2000. Large-scale methylation analysis of human genomic DNA reveals tissue-specific differences between the methylation profiles of genes and pseudogenes. Hum. Mol. Genet. 9, 2651–2663.
- Guevara, M.A., de Maria, N., Saez-Laguna, E., Velez, M.D., Cervera, M.T., Cabezas, J.A., 2017. Analysis of DNA cytosine methylation patterns using methylation-sensitive amplification polymorphism (MSAP). Methods Mol. Biol. 1456, 99–112.
- Guo, W., Schafer, S., Greaser, M.L., Radke, M.H., Liss, M., Govindarajan, T., Maatz, H., Schulz, H., Li, S., Parrish, A.M., Dauksaite, V., Vakeel, P., Klaassen, S., Gerull, B., Thierfelder, L., Regitz-Zagrosek, V., Hacker, T.A., Saupe, K.W., Dec, G.W., Ellinor, P.T., MacRe, C.A., Spallek, B., Fischer, R., Perrot, A., Ozcelik, C., Saar, K., Hubner, N., Gotthardt, M., 2012. RBM20, a gene for hereditary cardiomyopathy, regulates titin splicing, Nat. Med. 18, 766–773.
- Herrera, C.M., Bazaga, P., 2010. Epigenetic differentiation and relationship to adaptive genetic divergence in discrete populations of the violet *Viola cazorlensis*. New Phytol. 187, 867–876.
- Hirose, K., Shimoda, N., Kikuchi, Y., 2013. Transient reduction of 5-methylcytosine and 5hydroxymethylcytosine is associated with active DNA demethylation during

- regeneration of zebrafish fin. Epigenetics 8, 899-906.
- Jung, J., Moon, J.W., Choi, J.H., Lee, Y.W., Park, S.H., Kim, G.J., 2015. Epigenetic alterations of IL-6/STAT3 signaling by placental stem cells promote hepatic regeneration in a rat model with CCl4-induced liver injury. Int. J. Stem Cells 8, 79–89. Kerkel, K., Spadola, A., Yuan, E., Kosek, J., Jiang, L., Hod, E., Li, K., Murty, V.V., Schupf,
- N., Vilain, E., Morris, M., Haghighi, F., Tycko, B., 2008. Genomic surveys by methylation-sensitive SNP analysis identify sequence-dependent allele-specific DNA methylation. Nat. Genet. 40, 904–908.
- Kohli, R.M., Zhang, Y., 2013. TET enzymes, TDG and the dynamics of DNA demethylation. Nature 502, 472–479.
- Lu, Y., Rong, T., Cao, M., 2008. Analysis of DNA methylation in different maize tissues. J. Genet. Genomics 35, 41–48.
- Mandel, J.L., Chambon, P., 1979. DNA methylation: organ specific variations in the methylation pattern within and around ovalbumin and other chicken genes. Nucleic Acids Res. 7, 2081–2103.
- Marconi, G., Pace, R., Traini, A., Raggi, L., Lutts, S., Chiusano, M., Guiducci, M., Falcinelli, M., Benincasa, P., Albertini, E., 2013. Use of MSAP markers to analyse the effects of salt stress on DNA methylation in rapeseed (*Brassica napus* var. oleifera). PLoS One 8. e75597.
- Nabel, C.S., Jia, H., Ye, Y., Shen, L., Goldschmidt, H.L., Stivers, J.T., Zhang, Y., Kohli, R.M., 2012. AID/APOBEC deaminases disfavor modified cytosines implicated in DNA demethylation. Nat. Chem. Biol. 8, 751–758.
- Niehrs, C., Schafer, A., 2012. Active DNA demethylation by Gadd45 and DNA repair. Trends Cell Biol. 22, 220–227.
- Poon, K.L., Tan, K.T., Wei, Y.Y., Ng, C.P., Colman, A., Korzh, V., Xu, X.Q., 2012. RNA-binding protein RBM24 is required for sarcomere assembly and heart contractility. Cardiovasc. Res. 94, 418–427.
- Reyna-Lopez, G.E., Simpson, J., Ruiz-Herrera, J., 1997. Differences in DNA methylation patterns are detectable during the dimorphic transition of fungi by amplification of restriction polymorphisms. Mol Gen Genet 253, 703–710.
- Saze, H., Kakutani, T., 2011. Differentiation of epigenetic modifications between transposons and genes. Curr. Opin. Plant Biol. 14, 81–87.
 Schalkwyk, L.C., Meaburn, E.L., Smith, R., Dempster, E.L., Jeffries, A.R., Davies, M.N.,
- Schalkwyk, L.C., Meaburn, E.L., Smith, R., Dempster, E.L., Jeffries, A.R., Davies, M.N., Plomin, R., Mill, J., 2010. Allelic skewing of DNA methylation is widespread across the genome. Am. J. Hum. Genet. 86, 196–212.
- Schlosberg, C.E., VanderKraats, N.D., Edwards, J.R., 2017. Modeling complex patterns of differential DNA methylation that associate with gene expression changes. Nucleic Acids Res. 45, 5100–5111.
- Sha, A.H., Lin, X.H., Huang, J.B., Zhang, D.P., 2005. Analysis of DNA methylation related to rice adult plant resistance to bacterial blight based on methylation-sensitive AFLP (MSAP) analysis. Mol. Gen. Genomics. 273, 484–490.
- Sharma, R., Mohan Singh, R.K., Malik, G., Deveshwar, P., Tyagi, A.K., Kapoor, S., Kapoor, M., 2009. Rice cytosine DNA methyltransferases gene expression profiling during reproductive development and abiotic stress. FEBS J. 276, 6301–6311.
- Sharma, R., Vishal, P., Kaul, S., Dhar, M.K., 2017. Epiallelic changes in known stress-responsive genes under extreme drought conditions in *Brassica juncea* (L.) Czern. Plant Cell Rep. 36, 203–217.
- Shen, X., He, Z., Li, H., Yao, C., Zhang, Y., He, L., Li, S., Huang, J., Guo, Z., 2012. Distinct functional patterns of gene promoter hypomethylation and hypermethylation in cancer genomes. PLoS One 7, e44822.
- Smith, Z.D., Meissner, A., 2013. DNA methylation: roles in mammalian development. Nat. Rev. Genet. 14, 204–220.
- Takayama, K., Shimoda, N., Takanaga, S., Hozumi, S., Kikuchi, Y., 2014. Expression patterns of dnmt3aa, dnmt3ab, and dnmt4 during development and fin regeneration in zebrafish. Gene Expr. Patterns 14, 105–110.
- Tang, X.M., Tao, X., Wang, Y., Ma, D.W., Li, D., Yang, H., Ma, X.R., 2014. Analysis of DNA methylation of perennial ryegrass under drought using the methylation-sensitive amplification polymorphism (MSAP) technique. Mol. Gen. Genomics. 289, 1075–1084.
- Vanyushin, B.F., 2005. Enzymatic DNA methylation is an epigenetic control for genetic functions of the cell. Biochemistry (Mosc) 70, 488–499.
- Vos, P., Hogers, R., Bleeker, M., Reijans, M., van de Lee, T., Hornes, M., Frijters, A., Pot, J., Peleman, J., Kuiper, M., et al., 1995. AFLP: a new technique for DNA finger-printing. Nucleic Acids Res. 23, 4407–4414.
- Walsh, C.P., Bestor, T.H., 1999. Cytosine methylation and mammalian development. Genes Dev. 13, 26–34.
- Wang, Q., Ci, D., Li, T., Li, P., Song, Y., Chen, J., Quan, M., Zhou, D., Zhang, D., 2016. The role of DNA methylation in xylogenesis in different tissues of poplar. Front. Plant Sci. 7, 1003.
- Xu, Q., Zhang, Y., Sun, D., Wang, Y., Yu, Y., 2007. Analysis on DNA methylation of various tissues in chicken. Anim. Biotechnol. 18, 231–241.
- Yaish, M.W., Peng, M., Rothstein, S.J., 2014. Global DNA methylation analysis using methyl-sensitive amplification polymorphism (MSAP). Methods Mol. Biol. 1062, 285–298.
- Yang, C., Zhang, M., Niu, W., Yang, R., Zhang, Y., Qiu, Z., Sun, B., Zhao, Z., 2011. Analysis of DNA methylation in various swine tissues. PLoS One 6, e16229.
 Yang, C., Lu, X., Sun, H., Chu, W.H., Li, C., 2016. Analysis of genomewide DNA methy-
- Yang, C., Lu, X., Sun, H., Chu, W.H., Li, C., 2016. Analysis of genomewide DNA methylation reveals differences in DNA methylation levels between dormant and naturally as well as artificially potentiated pedicle periosteum of sika deer (*Cervus nippon*). J. Exp. Zool. B Mol. Dev. Evol. 326, 375–383.
- Zhang, D., Cheng, L., Badner, J.A., Chen, C., Chen, Q., Luo, W., Craig, D.W., Redman, M., Gershon, E.S., Liu, C., 2010. Genetic control of individual differences in gene-specific methylation in human brain. Am. J. Hum. Genet. 86, 411–419.
- methylation in human brain. Am. J. Hum. Genet. 86, 411–419.
 Zhao, Y., Chen, M., Storey, K.B., Sun, L., Yang, H., 2015. DNA methylation levels analysis in four tissues of sea cucumber *Apostichopus japonicus* based on fluorescence-labeled methylation-sensitive amplified polymorphism (F-MSAP) during aestivation. Comp. Biochem. Physiol. B Biochem. Mol. Biol. 181, 26–32.